



LAWRENCE  
LIVERMORE  
NATIONAL  
LABORATORY

# Demonstration of Tokamak Discharge Shutdown with Shell Pellet Payload Impurity Dispersal

E. M. Hollmann, P. B. Parks, D. Shiraki, N.  
Alexander, N. W. Eidietis, C. J. Lasnier, R. A.  
Moyer

June 26, 2019

Physical Review Letters

## **Disclaimer**

---

This document was prepared as an account of work sponsored by an agency of the United States government. Neither the United States government nor Lawrence Livermore National Security, LLC, nor any of their employees makes any warranty, expressed or implied, or assumes any legal liability or responsibility for the accuracy, completeness, or usefulness of any information, apparatus, product, or process disclosed, or represents that its use would not infringe privately owned rights. Reference herein to any specific commercial product, process, or service by trade name, trademark, manufacturer, or otherwise does not necessarily constitute or imply its endorsement, recommendation, or favoring by the United States government or Lawrence Livermore National Security, LLC. The views and opinions of authors expressed herein do not necessarily state or reflect those of the United States government or Lawrence Livermore National Security, LLC, and shall not be used for advertising or product endorsement purposes.

## Demonstration of Tokamak Discharge Shutdown with Shell Pellet Payload Impurity Dispersal

E.M. Hollmann<sup>1</sup>, P.B. Parks<sup>2</sup>, D. Shiraki<sup>3</sup>, N. Alexander<sup>2</sup>, N.W. Eidietis<sup>2</sup>, C.J. Lasnier<sup>4</sup>, and R.A. Moyer<sup>1</sup>

<sup>1</sup> University of California – San Diego, La Jolla, California 92093, USA

<sup>2</sup> General Atomics, San Diego, California 92186, USA

<sup>3</sup> Oak Ridge National Laboratory, Oak Ridge, Tennessee 37831, USA

<sup>4</sup> Lawrence Livermore National Laboratory, Livermore, California 94550, USA

The first rapid tokamak discharge shutdown using dispersive core payload deposition with shell pellets has been achieved in the DIII-D tokamak. Shell pellets are being investigated as a possible new path toward achieving tokamak disruption mitigation with both low conducted wall heat loads and slow current quench. Conventional disruption mitigation injects radiating impurities into the outer edge of the tokamak plasma, which tends to result in poor impurity assimilation and creates a strong outward temperature gradient with outward heat flow, thus requiring undesirable high-Z impurities to achieve low conducted heat loads. The shell pellet technique aims to produce a hollow temperature profile by using a thin low-ablation shell surrounding a dispersive payload, giving greatly increased impurity ablation (and radiation) rate when the payload is released in the plasma core. This principle was demonstrated successfully using OD = 3.6 mm, thickness = 40  $\mu\text{m}$  diamond shells holding boron powder. The pellets caused rapid (< 10 ms) discharge shutdown with low conducted divertor heat fluence ( $\sim 0.1 \text{ MJ/m}^2$ ). Confirmation of massive release of the boron powder payload into the plasma core was obtained spectroscopically. Some evidence for the formation of a hollow temperature profile during the shutdown was observed. These first results open a new avenue for disruption mitigation research, hopefully enabling development of highly effective methods of avoiding disruption wall damage in future reactor-scale tokamaks.

*Introduction.* – Major disruptions can occur in present tokamaks as a result of control or hardware system failure or operating too close to stability boundaries. They could pose an operational risk to future reactor-scale tokamaks like ITER due to wall damage [Hollmann2011]. Although extensive research has been devoted to improving tokamak plasma control systems, predicting tokamak plasma stability boundaries, and developing active disruption avoidance methods [Snipes2014, Humphreys2015], it is doubtful that it will be possible to avoid disruptions with 100% certainty, thus motivating the study of rapid shutdown techniques to quickly dissipate plasma stored energy in the event of an unavoidable disruption [Lehnen2015].

All rapid shutdown methods presently under consideration involve the injection of impurities to radiate away the plasma energy. A wide range of impurity delivery methods have been studied, including massive gas injection (MGI), cryogenic pellet injection (PI), and shattered cryogenic pellet injection (SPI) [Hollmann2015]. Good progress has been made in understanding the physics of tokamak disruptions and rapid shutdown, with shattered neon pellet injection presently considered the most promising baseline method for rapid shutdown of ITER [Commaux2016].

Despite the progress made on rapid shutdown research, shortcomings persist in present methods, partially due to poor impurity assimilation resulting from edge deposition and incomplete MHD mixing to assimilate impurities. It has been found that simultaneous reduction of induced vessel forces, conducted heat loads, and runaway electrons is challenging: higher-Z impurity injection tends to improve radiation efficiency, thus reducing conducted heat loads; but also causes more rapid electron temperature collapse (TQ) and more rapid current decay (CQ), thus increasing runaway electron (RE) production and induced vessel forces [Hollmann2015].

The dispersive shell pellet (DSP) concept seeks to increase impurity assimilation via the rapid delivery of a dispersive payload to the core of the discharge. High pressure gas [Hollmann2009] and dust [Parks2007] have been considered as dispersive payloads. An outer shell is used to hold the payload together and protect it from ablation at the plasma edge: edge ablation and cooling is undesirable because it can lead to current channel shrinking and TQ onset before most of the radiating impurities reach the core. In the ideal DSP shutdown, the pellet reaches the plasma core with minimal perturbation to the plasma, then releasing its payload rapidly and causing an inside-out TQ with inward flow of thermal energy into the core, giving the low conducted heat loads characteristic of high-Z shutdowns, but with the longer CQ and low induced vessel forces characteristic of lower-Z shutdowns [Izzo2017].

A challenge of the DSP shutdown method is designing a shell which is the correct thickness to survive to the plasma core. Ideally, the shell should be low-Z (for low radiation) but with high strength (to allow a thin wall). Previous attempts to demonstrate the DSP technique used polystyrene shells, which were unsuccessful; either not burning through in the core (for thick-walled shells) or breaking during launch (for thin-walled shells) [Hollmann2010]. Here, first successful demonstration of DSP shutdown with core impurity dispersal is presented, achieved by use of diamond shells.

*Experimental technique.* – The experiments were performed on the DIII-D tokamak [Luxon2002]. Medium-energy ( $W_{th} \approx 0.8$  MJ) neutral beam-heated deuterium H-mode lower-single null plasmas were used. Figure 1(a) shows a schematic of the pellet launcher. The pellets are launched using a pneumatic (helium propellant) pellet injector located at the low-field-side midplane. Propellant gas in the launcher is removed by two pumping ports to avoid the propellant perturbing the plasma. Initial pellet velocities of 80 – 250 m/s are measured with a light gate at the second pumping port. Additional essential diagnostics, shown in Fig. 1(b), include visible and ultraviolet spectrometers, a visible fast-framing camera, an infrared camera, a CO<sub>2</sub> interferometer, and photodiode arrays to measure total and soft x-ray (SXR) brightness. The shell pellets used here had 3.6 mm outer diameter and 40  $\mu$ m wall thickness. The wall was made of chemical vapor deposition (CVD) diamond. The payload was 21 mg of -325 mesh boron powder (44  $\mu$ m max OD).

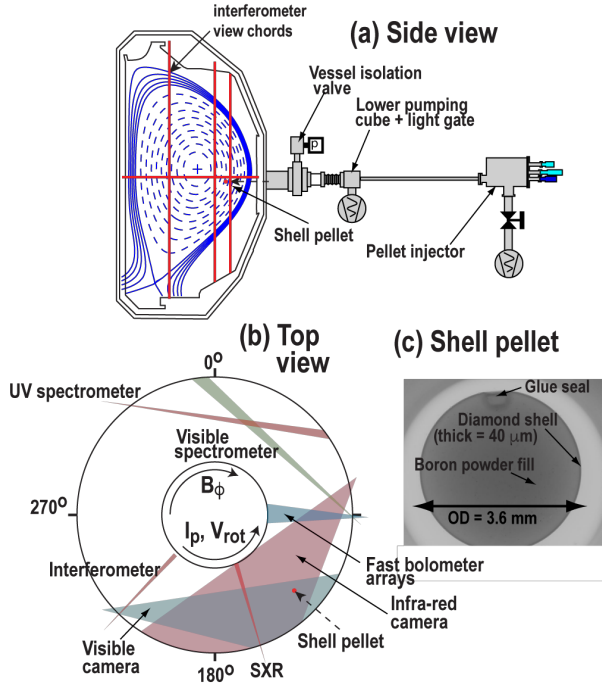


FIG. 1. (a) Schematic of pellet injector also showing equilibrium flux surfaces of target plasma; (b) tokamak top view showing key diagnostics; and (c) x-ray image of shell pellet.

*Demonstration of shell pellet shutdown.* – The main diagnostic used to track the pellet trajectory is the visible camera, which is used here with either B-II 412 nm (5 nm bandpass) or C-II 514 nm (4 nm bandpass) interference filters. Due to the high level of continuum emission from the pellet ablation plume plasma, the two filters gave similar results. Figure 2(a-h) shows visible images (with B-II filter) at different time steps,  $\Delta t \equiv t - t_{\text{impact}}$ , where  $t_{\text{impact}}$  is the time at which first ablation light from pellet-plasma interaction is observed. It can be seen that the pellet trajectory is fairly close (within  $\sim 1$  cm) of the expected straight-line vacuum trajectory (dashed line), allowing an estimate to be made of the pellet position in 3D space from the 2D images, giving the pellet minor radius,  $\rho = r/a$ , Fig. 2(i). The pellet light emission can initially be seen to be fairly localized to the pellet and to be extended along  $B$ , the magnetic field line direction. In Fig. 2(e), however, a cross-field dispersal of material can be seen, interpreted as shell burn-through and boron dust release. “Burn-through” is used here in the sense of ionization out of the neutral state (not in the usual sense of ionization to fully stripped ions).

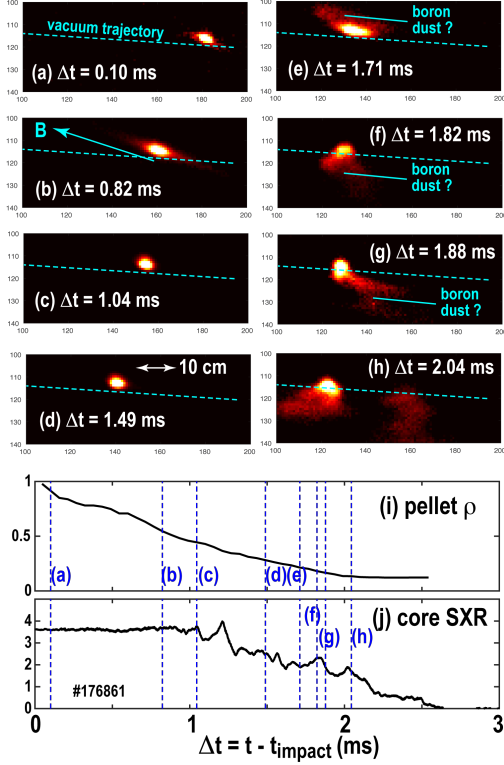


FIG. 2. (a-h). Visible images of shell pellet trajectory at different time steps, and (i) inferred pellet minor radius, and (j) core SXR brightness vs time.

Figure 3 compares time traces of pellet burn-through with modeling for a pellet with initial velocity  $\sim 230$  m/s. The experimental pellet trajectory is shown in Fig. 3(a), showing that pellet shells appear to burn through at  $\rho \sim 0.25$ , although pellet material goes farther, to  $\rho \sim 0.15$ , before stopping. Pellet brightness (integrated spatially over the image) is shown in Fig. 3(b); little difference is seen between B-II and C-II imaging (obtained by switching filters between repeat shots), consistent with continuum emission dominating the signal. There are spikes in emission seen when the pellet crosses the  $q = 2$  surface and again near the  $q = 3/2$  surface. These spikes are not understood at present. Previous small (weakly-perturbing) pellets observed emission dips at rational surfaces, associated with thermal energy depletion on rational surfaces [Houlberg1988]. Strongly perturbing (disrupting) Ar pellet experiments, however, exhibited emission spikes at rational surfaces, weaker for fast pellets and stronger for slow pellets, suggesting an instability which is enhancing cross-field heat transport [Hollmann2016]. The simulated pellet/payload trajectory is shown in Fig. 3(c), predicting shell burn-through around  $\rho \sim 0.3$ . For this simulation, recent calculations for carbon and boron ablation rates are used [Parks2018]. Ablated material is assumed to be deposited on flux surfaces over the width of the pellet diameter, and resulting plasma cooling due to ionization, dilution, and radiation is calculated from CRETIN [Scott2001]. The effect of cross-field heat transport is checked using a new kinetic model [Parks2018b] but is found to be small; for example, in the simulation of Fig. 3(c), including a radial thermal diffusivity of  $\chi_{\perp} = 1$  m<sup>2</sup>/s only increases the predicted shell penetration depth by  $\Delta\rho = 0.015$ . Pellet slowing is not

observed experimentally in the shell and is therefore neglected. After shell burn-through, the payload ablation is calculated in two limits: a solid boron limit, where the boron dust is treated as a single solid pellet of equivalent mass; and a boron dust limit, where dust ablation is calculated as if every grain were exposed to the full plasma heat flux (ignoring shadowing). As expected, B dust has a higher ablation rate, Fig. 3(d), but both B dust and solid B pass through the plasma without burning through. To match the observed B dust slowing, Fig. 3(a), dust slowing is added by ignoring ion drag and electric field forces and increasing the estimated ablation pressure gradient force across the grains by  $3\times$ . It can be seen from Fig. 3(c) that the resulting slowing matches the data, Fig. 3(a), although the experimental dust signal disappears at  $\Delta t \sim 2.5$  ms. This is presumably because the TQ comes to an end, Fig. 3(g), making dust difficult to see. “Control” experiments using solid plastic pellets of similar radius show that solid pellets of  $\sim$ mm size can be tracked even during the CQ, but it is likely that the  $<40 \mu\text{m}$  dust is not visible during the CQ.

The plume radius is shown in Fig. 3(e). It can be seen that the plume is initially broader in C-II, consistent with line emission becoming significant (relative to continuum) at the edges of the ablation plume. There is a rapid jump in plume radius which coincides with the observation of shell burn-through (dot-dashed vertical lines), suggesting that this jump is due to dust dispersal. Total radiated power measured at toroidal angles  $\phi = 90^\circ$  and  $\phi = 210^\circ$  are shown in Fig. 3(f). It can be seen that the radiated power is asymmetric toroidally. Figure 3(g) shows core SXR brightness and Fig. 3(h) shows plasma current. It can be seen that the TQ begins after the pellet crosses the  $q = 3/2$  surface, and payload dispersal then occurs during the TQ. Significant plasma cooling therefore already takes place even before payload release.

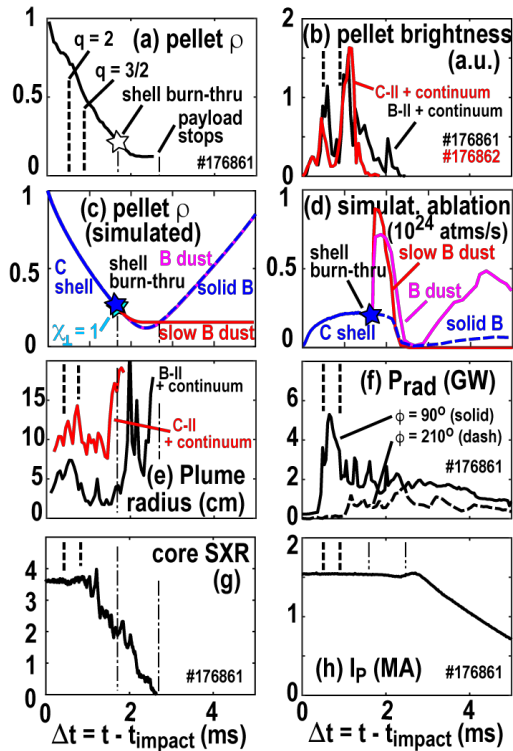


FIG. 3. Time traces of fast ( $v \sim 230$  m/s) shell pellet shutdown showing (a) pellet minor radius, (b) ablation plume brightness, (c) simulated pellet minor radius, (d) simulated ablation rate, (e) ablation plume characteristic radius, (f) radiated power, (g) core SXR, and (h) plasma current.

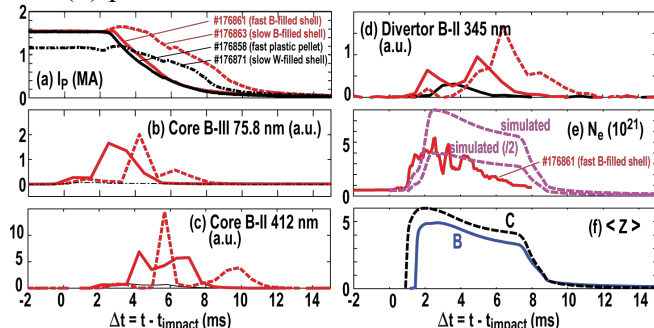


FIG. 4. Time traces of (a) plasma current, (b) core B-III line brightness, (c) core B-II line brightness, (d) divertor B-II line brightness, (e) total electron number for pellets with and without boron payload, and (f) mean charge state from 0D model.

Confirmation of boron dispersal in the plasma during the TQ is obtained spectroscopically, as shown in Fig. 4. Figure 4(a) shows time traces of plasma current for four shots – red curves are boron-filled shell pellets, while the black curves are examples of boron-free controls – a solid plastic pellet, and a tungsten powder-filled shell pellet. Core boron line emission rises before the CQ onset for the boron-filled pellets, Fig. 4(b), consistent with boron being released during the TQ. Visible boron line emission rises later, during the CQ, Figs. 4(c,d) consistent with recombination of boron into low-lying charge states during the CQ. Figure 4(e) shows the total plasma electron number reconstructed from interferometer view chords. The upper dashed line shows the electron number simulated from 0D ionization/recombination modeling of the injected atoms (KPRAD) [Hollmann2008]. It can be seen that the measurement is about  $2\times$  lower than predicted, suggesting incomplete assimilation of released boron dust, although toroidal asymmetries cannot be ruled out. Figure 4(f) shows the mean charge states of B and C predicted by the 0D modeling. It can be seen that fully stripped ions can be achieved during the TQ, with mean charge state dropping during the CQ.

Some preliminary evidence of an inside-out TQ forming during DSP shutdown was obtained from Thomson scattering data, shown in Fig. 5. In Fig. 5(a), it can be seen that the temperature profile is hollow at time  $\Delta t = +1$  ms. Due to significant jitter (of order 1 ms) in shell pellet arrival time, only this isolated example of a TQ  $T_e$  profile was obtained. Additionally, the time  $\Delta t = +1$  ms is slightly prior to shell burn-through, so the hollowing does not appear to be due to the payload dispersal. However, this data does demonstrate that inside-out  $T_e$  profiles are achievable, and can hopefully be made even more hollow (deeper) with less perturbing shells.

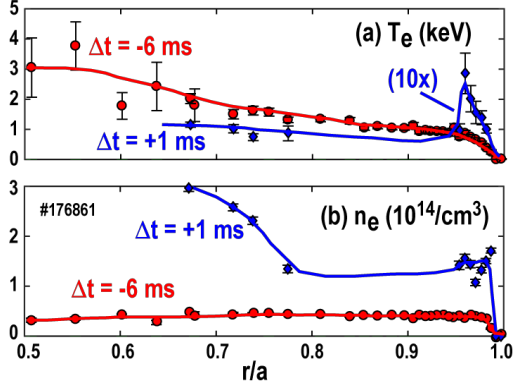


FIG. 5. Radial profiles of (a) electron temperature (with blue curve scaled  $\times 10$ ) and (b) electron density measured before and after pellet impact.

*Global characteristics.*- A qualitative overview of typical OD disruption mitigation metrics for DSP shutdowns are shown in Fig. 6 as a function of initial pellet velocity. Fig. 6(a) shows the height of the CQ  $I_p$  spike, which is interpreted qualitatively as the degree of current flattening which occurs at CQ onset, and is therefore inversely linked to the level of TQ MHD. A low  $I_p$  spike is desirable, as it indicates low MHD mixing of impurities and is associated with better impurity assimilation. CQ duration is shown in Fig. 6(b) - it can be seen that there is a clear decreasing trend in CQ duration with pellet velocity. This trend is undesirable, as it is desired to achieve long CQ duration with good heat load mitigation. Inner divertor leg heat fluence, from IR thermography, is shown in Fig. 6(c); this gives a qualitative picture of the degree of conducted heat load mitigation, showing excellent heat load mitigation (comparable to neon SPI but using lower Z impurities). Integrated halo current amplitude is shown in Fig. 6(d); this gives a rough picture of the level of (undesirable) halo current vessel forces. Integrated CQ hard x-ray (HXR) signals are shown in Fig. 6(e); these reflect the level of (undesirable) runaway electron (RE) generation during the shutdown. Surprisingly, the DSP shutdowns can form REs, even with low Z injection, indicating very rapid thermal collapse on good flux surfaces, consistent with very rapid core impurity deposition. The colored bands in Fig. 6(a-e) show approximate equivalent values for shutdowns with Ar PI, Ne SPI, and D<sub>2</sub> SPI. These are not for the same target plasma, being taken on different run days, so are intended for rough comparison only. Fig. 6(f) shows the estimated shell burn-through radius as a function of initial pellet velocity.

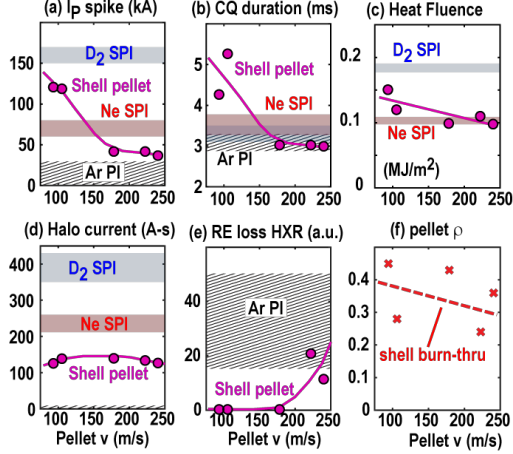


FIG. 6. 0D disruption mitigation metrics as a function of pellet initial velocity showing (a)  $I_P$  spike height, (b) CQ duration, (c) inner strike point conducted heat fluence, (d) integrated halo current amplitude, (e) runaway electron prompt loss level, and (f) shell burn-through radius.

*Summary and conclusion.*- This work presents first demonstration of the shell pellet concept for core payload dispersal during rapid shutdown for tokamak disruption mitigation. This differs significantly from conventional disruption mitigation, where impurities are dominantly mixed into the plasma by MHD processes. Many encouraging features were observed, including core release of boron dust and evidence for rapid slowing of the dust payload after being released. Assimilation of injected material (shell + payload) appeared to be quite good ( $>50\%$ ). Low conducted heat loads, low  $I_P$  spike, and low halo currents were observed at higher pellet velocities. Undesirable trends included strong plasma perturbation by the shell (indicating a need for even lower Z shells), toroidally localized TQ radiation, short CQ duration, and RE formation. Overall, the disruption mitigation characteristics of these prototype shell pellets are quite good, giving reason to believe that even better results can be obtained with future, more optimized, designs.

The authors wish to thank L. Chousal, J. Kulchar, A. Horton, and D. Ayala for assistance with design, testing, and installation of the pellet injector and J. Herfindal, A. Lvovsky, I. Bykov, M. van Zeeland, F. Glass, Y. Zhu, and D. Thomas for diagnostic support and A. Hyatt, H. Torreblanca for operations support. This work was supported by the U.S. Department of Energy under Grants No. DE-FG02-07ER54917, DE-FC02-04ER54698, D E A C 5 2 - 0 7 N A 2 7 3 4 4 and DE-AC05-00OR22725. DIII-D data shown in this paper can be obtained in digital format by following the links at <https://fusion.gat.com/global/D3D DMP>.

**Disclaimer:** This report was prepared as an account of work sponsored by an agency of the United States Government. Neither the United States Government nor any agency thereof, nor any of their employees, makes any warranty, express or implied, or assumes any legal liability or responsibility for the accuracy, completeness, or usefulness of any information, apparatus, product, or process disclosed, or represents that its use would not infringe privately owned rights. Reference herein to any specific commercial product, process, or service by trade name, trademark, manufacturer, or otherwise does not necessarily constitute or imply its endorsement,

recommendation, or favoring by the United States Government or any agency thereof. The views and opinions of authors expressed herein do not necessarily state or reflect those of the United States Government or any agency thereof.

## References

- [Hollmann2011] E.M. Hollmann, G. Arnoux, N. Commaux, et al., *J. Nucl. Mater.* **415**, S27 (2011).
- [Snipes2014] J.A. Snipes, S. Bremond, D.J. Campbell, et al., *Fus. Eng. Design* **89**, 507 (2014).
- [Humphreys2015] D. Humphreys, G. Ambrosio, P. de Vries, et al., *Phys. Plasmas* **22**, 021806 (2015).
- [Lehnen2005] M. Lehnen, K. Aleynikova, P.B. Aleynikov, et al., *J. Nucl. Mater.* **463**, 39 (2015).
- [Hollmann2015] E.M. Hollmann, P.B. Aleynikov, T. Fulop, et al., *Phys. Plasmas* **22**, 021802 (2015).
- [Commaux2016] N. Commaux, D. Shiraki, L.R. Baylor, et al., *Nucl. Fusion* **56**, 046007 (2016).
- [Hollmann2009] E.M. Hollmann, A.N. James, P.B. Parks, et al., “Atomic Processes in Plasmas,” *AIP Conf. Proc.* **1161**, 65 (2009).
- [Parks2007] P.B. Parks, “Dust ball pellets for disruption mitigation,” Invention Disclosure DOE Case no. S-113-472 (2007).
- [Izzo2017] V.A. Izzo and P.B. Parks, *Phys. Plasmas* **24**, 060705 (2017).
- [Hollmann2010] E.M. Hollmann, N. Commaux, N.W. Eidietis, et al., *Phys. Plasmas* **17**, 056117 (2010).
- [Luxon2002] J.L. Luxon, *Nucl. Fusion* **42**, 614 (2002).
- [Houlberg2018] W.A. Houlberg, S.L. Milora, and S.E. Attenberger, *Nucl. Fusion* **28**, 595 (1988).
- [Hollmann2016] E.M. Hollmann, N. Commaux, R.A. Moyer, et al., *Nucl. Fusion* **57**, 015008 (2016).
- [Parks2018] P.A. Parks, “The ablation rate of some low-Z pellets with a kinetic model for the degradation of the incident plasma electrons in the surrounding ablation cloud,” to be submitted to *Phys. Plasmas* (2018).
- [Scott2001] H.A. Scott, *J. Quant. Spectrosc. Radiat. Transfer* **71**, 689 (2001).
- [Parks2018b] P.A. Parks and E.M. Hollmann, “A kinetic model for plasma cooling induced by pellet injection,” to be submitted to *Phys. Plasmas* (2018).
- [Hollmann2008] E.M. Hollmann, P.B. Parks, and H.A. Scott, *Contr. Plasma Phys.* **48**, 260 (2008).